Journal of Fractional Calculus and Applications,
Vol. 3. July 2012, No.1, pp. 1–15.
ISSN: 2090-5858.
http://www.fcaj.webs.com/

STABILITY ANALYSIS OF THE FRACTIONAL-ORDER $RL_\beta C_\alpha$ CIRCUIT

A. G. RADWAN

Abstract. In this paper, we will introduce a generic study of the series $RL_\beta C_\alpha$ circuit in the fractional-order domain. The added two fractional-order parameters (α,β) increase the degree of freedom in the design over the conventional RLC circuit. Therefore, the total number of parameters becomes five instead of three which means that the conventional RLC theorems and analyses represent a point $(1, 1)$ in the α-β plane. Stability study in the fractional plane (F) and in the physical s-plane for different cases will be introduced. The effect of the circuit values (R,L,C) on the poles of the characteristic equation will be investigated for each case. The analytical formula of the poles in case of equal fractional-orders will be also presented. Many examples showing the magnitude and phase responses for the fractional-order $RL_\beta C_\alpha$ low-pass filter (LPF) will be discussed to validate the previous stability analysis.

1. Introduction

Although fractional calculus was investigated during the same time period of the conventional calculus, but the lack of applications and its complexity analysis were the main reasons for the delay in the development of research in the area of fractional calculus. [1]-[2]. Recently and during the last five decades, the fractional calculus research topics in different fields were investigated again due to the discovery of its major advantages over the conventional modeling techniques. In addition, the behavior of many natural-phenomena as investigated by scientists in numerous fields depends on global memory and the ability to use information from its previous history which can be modeled as fractional-order differential equations. As known, to calculate the fractional-order derivative of a certain function you need to know all the history of this function unlike the integer derivatives which need only few previous values for calculation. Besides the advantage of long-memory dependence of the fractional-order modeling, the extra fractional-order parameters increase the degree of freedom of the system which can be used for flexible design, investigation of new fundamentals, best experimental fitting, optimization, and adding extra constraints.
The influences of fractional-order modeling are discussed in many established fields

2000 *Mathematics Subject Classification.* 34A12, 34A30, 34D20.
Key words and phrases. Fractional-order differential equations, stability, fractional-order circuit theory, fractional-order stability, RLC circuit, fractional-order filter.
Submitted Nov., 11, 2011. Accepted Jan, 10, 2012, Published July 1, 2012.

and generate new concepts such as the fractional-order circuit theories [3]-[4], control theory [5]-[6], bioengineering [7]-[8], electromagnetics and Smith chart [9]-[10], chaotic systems [11]-[12], bifurcation maps [13], digital designs [14] and modeling of botanical systems [15]. The main reason for the huge research interests in the area of fractional-calculus comes from the approximation techniques for solving the fractional-order differential equations [16]-[17], stability analysis [18]-[19], and also from the numerous trials for the physical realizations of the fractional-element [20]-[27].

In this paper, we will restudy the series RLC circuit in the fractional-order domain and discuss the stability issues for different cases which are required for the design of the fractional-order filters and oscillators. Many numerical examples will be introduced to validate the analytical study. In addition the magnitude and phase responses will be presented for several cases.

2. Fractional-order $RL_\beta C_\alpha$ circuit

The series fractional-order$RL_\beta C_\alpha$ is shown in Figure 1, where the current flowing in this circuit is given by

$$E(t) = Ri(t) + \frac{1}{C\Gamma(\alpha)} \int_0^t \frac{i(\sigma)}{(t-\sigma)^{1-\alpha}} d\sigma + L \frac{d^\beta i(t)}{dt^\beta} \tag{1}$$

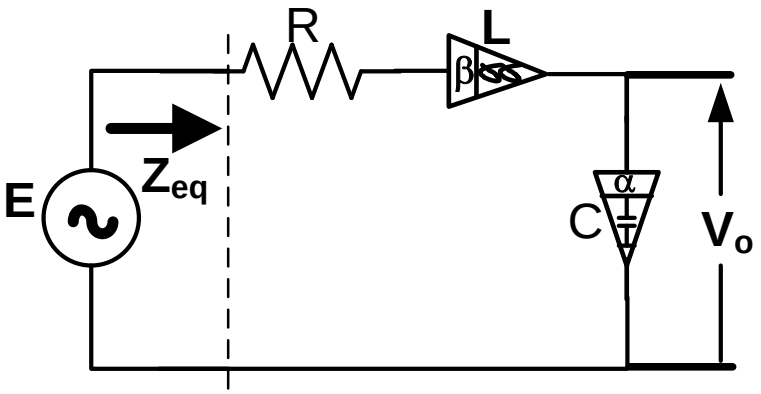

Figure 1. The fractional-order $RL_\beta C_\alpha$ circuit

Based on the Laplace transform, and assume zero initial conditions, the input impedance of the $RL_\beta C_\alpha$ circuit in the s-plane is

$$Z(s) = \frac{E(s)}{I(s)} = R + s^\beta L + \frac{1}{s^\alpha C} \tag{2}$$

Therefore, the input-output relationship of the shown fractional-order low-pass filter in the frequency domain is given by

$$G(s) = \frac{V_o(s)}{E(s)} = \frac{1}{1 + s^\alpha RC + s^{\alpha+\beta} LC} \tag{3}$$

The frequency response of this filter was discussed before in [4] when $\alpha = \beta$ and many interesting fundamentals are shown only in the fractional-order and not in

the conventional RLC circuit. The stability analysis of the circuit is considered the first step for designing and analysis. For simplicity, assume that

$$\begin{aligned} LC &= \tau^{\alpha+\beta} \\ RC &= k\tau^{\alpha} \\ \tau &= \big(LC\big)^{\frac{1}{\alpha+\beta}} \\ k &= \frac{RC}{(LC)^{\frac{\alpha}{\alpha+\beta}}} \\ y &= \tau s \end{aligned} \tag{4}$$

Hence (3) can be rewritten as

$$\begin{aligned} G(y) &= \frac{V_o(y)}{E(y)} \\ &= \frac{1}{1+ky^{\alpha}+y^{\alpha+\beta}} \end{aligned} \tag{5}$$

From the general theorems of the fractional-order oscillators discussed in [3], this system will oscillate with frequency ω_o if and only if the following condition is met

$$\begin{aligned} \omega_o &= \big(\tfrac{-Rsin(0.5\alpha\pi)}{Lsin(0.5(\alpha+\beta)\pi)}\big)^{\frac{1}{\beta}} \\ &= \big(\tfrac{-sin(0.5(\alpha+\beta)\pi)}{RCsin(0.5\beta\pi)}\big)^{\frac{1}{\alpha}}, \alpha+\beta>2 \end{aligned} \tag{6}$$

From the previous equation, it is clear that the frequency ω_o is proportional to the factor $(\frac{1}{RC})^{\frac{1}{\alpha}}$ which means that if $\alpha = 0.2$, this term will be $(\frac{1}{RC})^5$. Therefore, one of the main advantages of using fractional-order elements is that the frequency of oscillation can be controlled from very low frequencies up to very high frequencies only by choosing the appropriate value of α as shown from Figure 2.

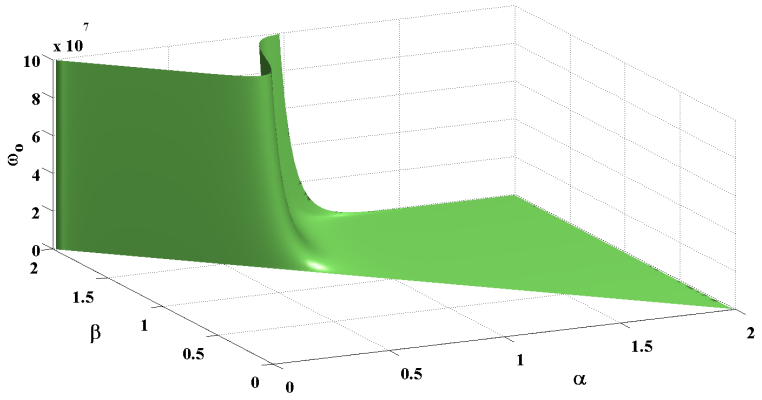

FIGURE 2. The frequency of oscillation ω_o surface versus the $\alpha-\beta$ plane when $LC = 10^{-6}$

Generally, the system has four different cases as follows (assume $\alpha < 1$):

(1) $\beta \in (0, 1-\alpha]$: The system poles are in the non-physical s-plane (no poles exist in the s-plane).
(2) $\beta \in (1-\alpha, 1)$: The poles enter the physical s-plane. The system poles in this case conditionally depend on k and cant oscillate. Therefore, the system has poles in the s-plane when $k \in [0, k_{max}]$ where k_{max} is given by

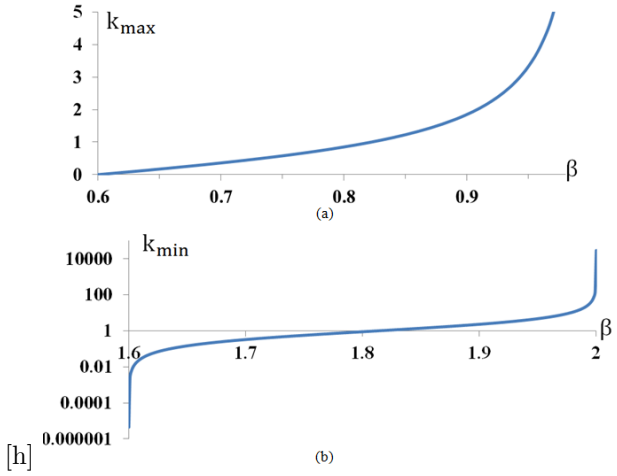

[h]

FIGURE 3. The values of k_{max} and k_{min} versus β

$$k_{max} = \frac{-sin((\alpha+\beta)\pi)}{\left(sin^{\beta}(\beta\pi)sin^{\alpha}(\alpha\pi)\right)^{\frac{1}{\alpha+\beta}}}, \alpha+\beta > 1 \tag{7}$$

(3) $\beta \in [1, 2-\alpha)$: The poles always in the stable region of the s-plane are (unconditionally stable) whatever the value of k.

(4) $\beta \in [2-\alpha, 2]$: The poles initially ($k = 0$) located in the unstable region of s-plane and as k increases as the poles move toward the stable region. Then, the system will be stable if the value of $k \in [k_{min}, \infty)$ where k_{min} is given by

$$k_{min} = \frac{-sin(0.5(\alpha+\beta)\pi)}{\left(sin^{\beta}(0.5\beta\pi)sin^{\alpha}(0.5\alpha\pi)\right)^{\frac{1}{\alpha+\beta}}}, \alpha+\beta > 2 \tag{8}$$

Interval $\beta \in (0.6, 1]$			**Interval $\beta \in [1.6, 2]$**	
β	k_{max}		β	k_{min}
0.61	0.03324		1.6	zero
0.65	0.171259		1.65	0.146745
0.7	0.360143		1.7	0.328028
0.75	0.579143		1.75	0.563201
0.8	0.851794		1.8	0.889658
0.85	1.229319		1.85	1.391082
0.9	1.852462		1.9	2.305292
0.95	3.336444		1.95	4.726764
1	∞		2	∞

TABLE 1. The values of k_{max} and k_{min} versus β

Note that, the value k_{min} calculated in (8) has the same condition of oscillation given before in (6). Table 1 and Figure 3 show the critical values of k for different values of β when $\alpha = 0.4$. Therefore, the range of β for positive k_{max} and k_{min} from (7) and (8) will be $(0.6, 1)$ and $(1.6, 2)$ respectively. It is clear from the figures

that k_{max} and k_{min} scan all positive values from 0 up to ∞. Note that the y-axis in Figure 3(b) is log-scale to illustrate the sensitivity effect of β on the value of k_{min}.

3. Stability analysis in the F plane

The poles of this system can be calculated from the characteristic equation $1 + ky^\alpha + y^{\alpha+\beta} = 0$ and using the proposed technique in [18]. Figure 4 shows the poles in the F-plane when $\beta = m\alpha$ and $F = y^\alpha = (s\tau)^\alpha$ where the number of poles is $(m + 1)$ in the F-plane. Four different cases are discussed at $m = 1, 2, 3$, and 4 in the range of $k \in [0.005, 50]$.

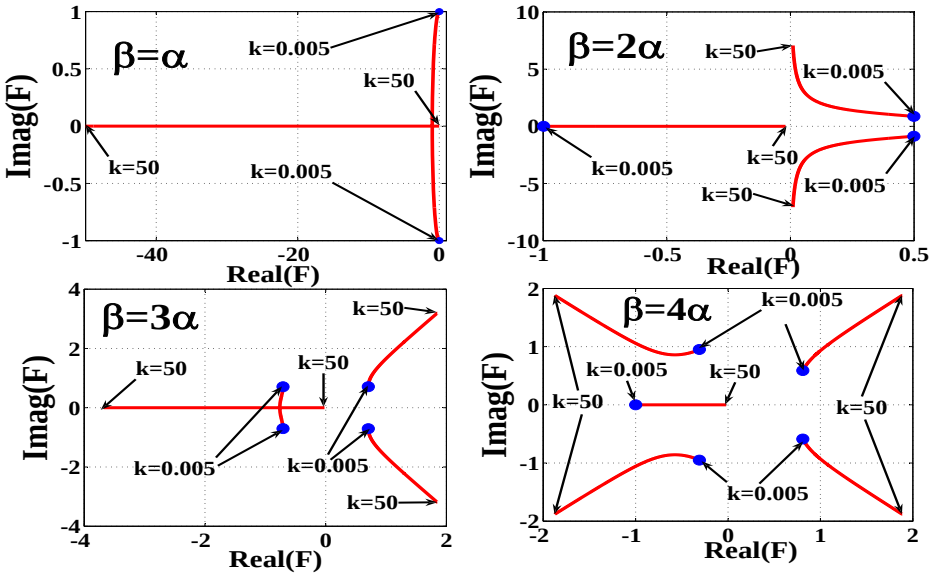

Figure 4. Poles in the F-plane of the characteristic equation $1 + kF_1 + F_1^{m+1} = 0$, where $F_1 = (s\tau)^\alpha$ and $\beta = m\alpha$ in case of $m = 1, 2, 3$, and 4

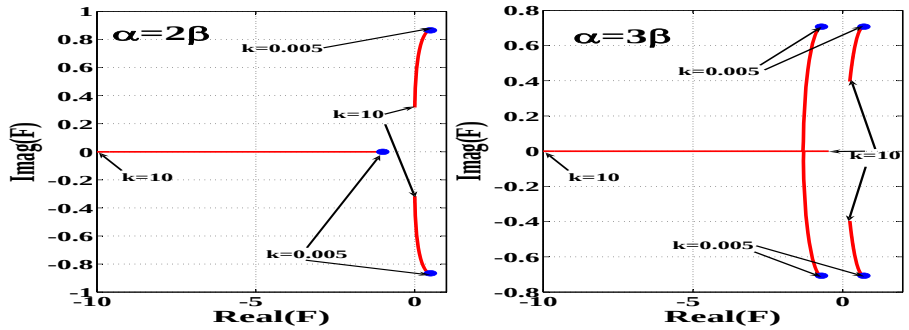

Figure 5. Poles in the F-plane of the characteristic equation $1 + kF_2^m + F_2^{m+1} = 0$, where $F_2 = (s\tau)^\beta$ and $\alpha = m\beta$ in case of $m = 2$ and 3

When $\alpha = \beta$, the two poles always exist in the left half F-plane. However, in the coming cases, there are two poles in the right half F-plane and other poles one at $m = 2$, two at $m = 3$, and three at $m = 4$ lie on the left-half F-plane. The poles in the F-plane when $\alpha = m\beta$ in case of $m = 2$ and $m = 3$, are shown in Figure 5.

4. Stability analysis in the physical s-plane

The stability analysis discussion in the F-plane has no meaning without mapping these poles into the physical s-plane. When $F = s^{\alpha}$, the physical s-plane is confined between the two angles $\angle F = \pm\alpha\pi$, where the mapping area depends on α. For the conventional case, the F-plane will be the same as s-plane.

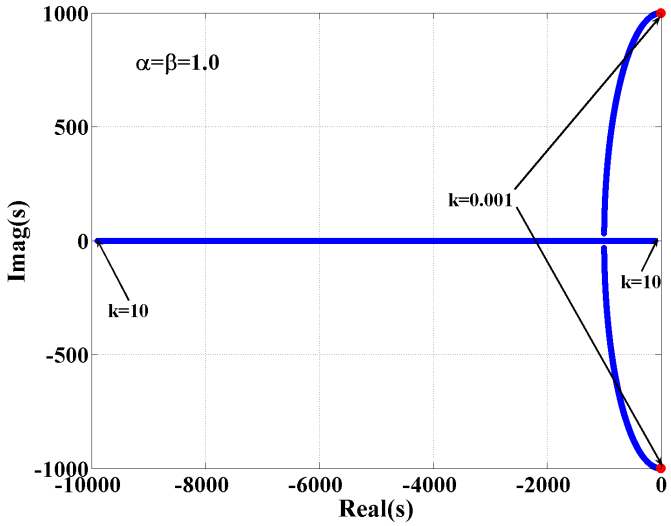

Figure 6. Poles in the conventional s-plane when the parameter $k \in [0, 10]$

4.1. **Conventional case** $(\alpha = \beta = 1.0)$**.** For the conventional case when$(\alpha = \beta = 1.0)$ and $LC = 10^{-6}$, the poles in the s-plane are shown in Figure 6. There are three different cases:

(1) If $k = 0$, the system will oscillate with frequency $\omega_o = \frac{1}{\sqrt{LC}} = 1000 Rad/Sec.$
(2) If $k < 2$, the two poles (conjugate) are decaying as k increases, and the poles' frequency is less than 1000.
(3) If $k \geq 2$, the two poles are negative real values and no frequency component exists.

4.2. **Fractional-order stability analysis** $(\alpha, \beta \neq 1.0)$**.** Without loss of generality, let $\beta = m\alpha$ where m is real value and can cover all the range of β. Then using $F = y^{\alpha}$ the characteristic equation will be given by

$$1 + kF + F^{m+1} = 0 \tag{9}$$

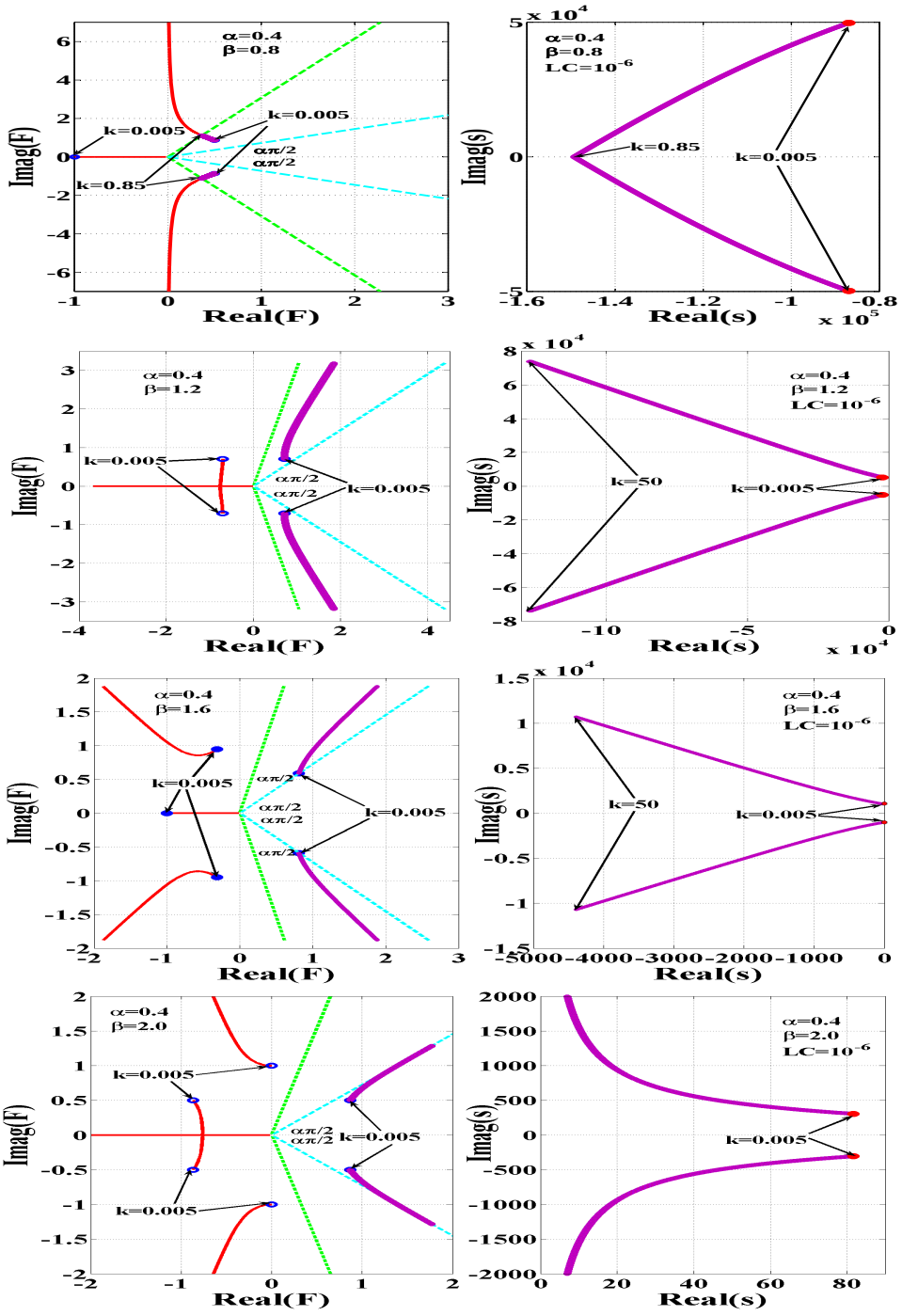

FIGURE 7. Poles in the F and s planes when $k \in [0.005, 50]$

The previous equation is a polynomial, and has $(m+1)$ roots in the F-plane. In addition, it depends only on k and m values. In order to get the poles in the s-plane, a conversion-scheme must be applied. This conversion from the F-plane into the s-plane can be divided into two steps. The first step is to select the poles in the F-plane which is inside the conventional s-plane. This can be achieved by picking-up all the poles whose angle satisfies the following relationship:

$$|\angle F_*| \leq \alpha\pi \tag{10}$$

Then, these poles can be mapped into the s-plane through

$$s_* = \frac{F_*^{\frac{1}{\alpha}}}{\tau} = \frac{F_*^{\frac{1}{\alpha}}}{(LC)^{\frac{1}{\alpha+\beta}}} = (\frac{F_{*s}}{\sqrt[m+1]{LC}})^{\frac{1}{\alpha}} \tag{11}$$

Figure 7 shows the poles in both the F-plane and the s-plane for four different cases when $\alpha = 0.4$ and $LC = 10^{-6}$. Since $\alpha < 1$, the physical s-plane will be a part of the F-plane. As known, the four quadrants in the s-plane are separated by the angles $\theta_s = 0, \pm\pi/2$,and $\pm\pi$ (overlapped two lines). The angle $\theta_s = 0$ is the same as $\theta_F = 0$. However, the internal dotted lines (with cyan color) represent the lines $\theta_s = \pm\pi/2$, $s = \pm j\omega$ and the external dotted lines (with green color) represent the $\theta_s = \pm\pi$ (the negative real-axis, which are identical) in the s-plane. For the following cases, we will fix $\alpha = 0.4$ and discuss the effect of β on the poles of different systems. For $\beta = \alpha = 0.4 < 0.5$ all the poles will be outside the physical s-plane. Thus, no physical poles will exist in the s-plane. As β increases, the poles start to enter the physical s-plane as shown in Figure 6.

When $\beta = 2\alpha = 0.8$, the poles exist in the physical s-plane for a very limited range of $k \in [0, 0.85]$ as shown in Figure 7(a) by the purple lines. When $k = 0$, only two from the three poles located between the dotted lines are located in the F-plane. These two poles are transformed into two conjugate poles in the s-plane (red circles). As k increases, the poles in the F-plane move away from the dotted lines and the third real pole move right toward zero. In the s-plane, as k increases ($k < 0.85$) the conjugate poles in the s-plane become closer. Moreover, the poles frequency decreases until the poles overlap at $k = 0.85$. When $k > 0.85$, the system is stable but there is no poles in the physical s-plane.

Figure 7(b) shows the poles in case of $\beta = 3\alpha = 1.2$, where two poles from the four poles are always between the dotted lines in the F-plane. Therefore, at any value of k there are two conjugate poles in the s-plane which are always located in the second and third quadrants. Since there is no intersection between the poles and the cyan dotted lines ($s = \pm j\omega$), then the system cannot oscillate for any positive k. Another difference between this case and the previous one is as k increases the distance between the conjugate poles in the s-plane increases, i.e. the poles frequency increases as k increases.

When $\beta = 4\alpha = 1.6$, as in the previous case two poles are always inside the physical s-plane, however the system can oscillate with frequency $\omega_o = \frac{1}{\sqrt{LC}} = 1000 Rad/Sec$ when $k = 0$, which is clear from the intersection between the poles (purple lines) and the cyan dotted lines in the F-plane as shown in Figure 7(c). In the s-plane, the poles starts from the $\pm j\omega$ axis and separates away as k increases. If $\beta = 5\alpha = 2.0$, there are six poles in the F-plane for each value of k, two of them always located between the dotted lines. But, they are inside the inner dotted lines

(cyan color), which will be mapped into the unstable region in the s-plane as shown in Figure 7(d).

In the integer-order case ($\alpha = \beta = 1$) the properties of the poles depend on the parameter k only. However, in the fractional-order case, the two extra parameters which are added affect the system poles. From Figure 7 ($\alpha = 0.4$), many systems which have only two conjugate-poles are introduced, and none of them have real poles. They are conveying different properties such as: stable or conditionally stable or unstable. Moreover, the poles frequency increases or decreases as k increases and with different ranges.

Five different cases are discussed for this fractional-order system as in Figure 7, which are:

(1) No poles inside the s-plane as in the case when $\beta = \alpha = 0.4$ independent of k
(2) Poles inside the s-plane exist only in a certain range of k, as in the case when $\beta = 2\alpha = 0.8$
(3) Poles exist in the s-plane independent of k without the possibility of free oscillations $|\angle\theta_s| > \pi/2$, as in $\beta = 3\alpha = 1.2$
(4) Poles exist in the s-plane independent of k with the possibility of free oscillations $|\angle\theta_s| > \pi/2$, as in $\beta = 4\alpha = 1.6$
(5) Poles always inside the left-half s-plane independent of k, as in the case when $\beta = 5\alpha = 2.0$

4.3. **When $\alpha = \beta$ with Fixed k.** In the case when $\alpha = \beta$, the input output relationship will be reduced to:

$$G(s) = \frac{V_o(s)}{E(s)} = \frac{1}{1 + k(\tau s)^\alpha + (\tau s)^{2\alpha}} = \frac{1}{1 + kF + F^2} \tag{12}$$

Where $LC = \tau^{2\alpha}$, $RC = k\tau^\alpha, \tau = (LC)^{\frac{1}{2\alpha}}, k = \frac{RC}{\sqrt{LC}} = R\sqrt{\frac{C}{L}}, F = (\tau s)^\alpha$. Therefore, the poles in the F and s planes can be given by

$$F = \frac{1}{2}(-k \pm \sqrt{k^2 - 4}) = (\tau s)^\alpha = s^\alpha \sqrt{LC} \tag{13}$$

$$s_* = \big(\frac{1}{2\sqrt{LC}}(-k \pm \sqrt{k^2 - 4})\big)^{\frac{1}{\alpha}} = |s_1|^{\frac{1}{\alpha}} e^{\pm \frac{j\theta_s}{\alpha}} \tag{14}$$

For $k < 2$, the poles in the F-plane are conjugate poles, but in the case of $k \geq 2$ the poles will be located in the negative real F-axis. When $\alpha < 1$, the negative real F-axis will be always outside the physical s-plane. Thus, poles could appear in the s-plane only when $k < 2$. Figure 8, illustrates the poles locations in the s-plane for four different cases of k and when $\alpha = \beta$. In each case of k, there is a certain range of $\alpha_{min} < \alpha < 1$, at which the system has poles in the s-plane. For example, when $k = 1$ the poles in the s-plane are as follows:

$$s_* = \big(\frac{1}{2\sqrt{LC}}(-1 \pm j\sqrt{3})\big)^{\frac{1}{\alpha}} = \big(\frac{e^{\pm \frac{j2\pi}{3}}}{\sqrt{LC}}\big)^{\frac{1}{\alpha}} \tag{15}$$

Due to the boudary phase condition $|\theta_s| < \pi$, the poles will appear if and only if $\alpha > \alpha_{min} = \frac{2}{3}$ as shown in Figure 8. Generally, as the value of k increases, the range of $\alpha = \beta$ for which poles exist in the physical s-plane decreases. As k approaches 2, this range shrinks into one point at $\alpha = 1$. In addition, the shape

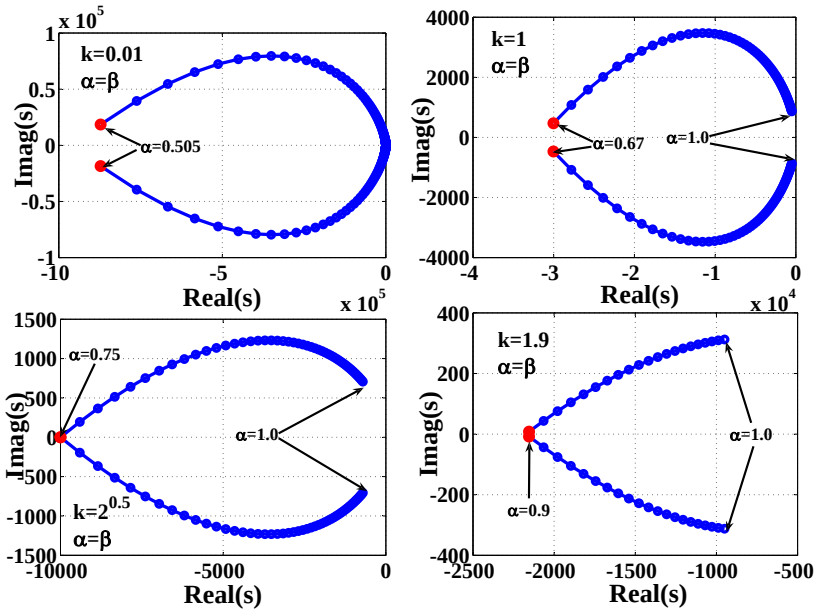

FIGURE 8. Range of the fractional-order at which poles exist in the s-plane when $\alpha = \beta$ for different cases of constant k

of the poles has a peak at a certain value of $\alpha = \alpha_*$ at which the tangent will be horizontal. The poles can be rewritten in the form

$$s_* = |s_1|^{\frac{1}{\alpha}}(cos(\frac{\theta_s}{\alpha}) \pm jsin(\frac{\theta_s}{\alpha})) = \sigma \pm j\omega \tag{16}$$

Then at $\alpha = \alpha_*$, $\partial\omega/\partial\alpha = 0$, therefore

$$tan(\frac{\theta_s}{\alpha_*}) = -\frac{\theta_s}{ln(|s_1|)} \tag{17}$$

$$\alpha_* = \frac{\theta_s}{tan^{-1}(\frac{-\theta_s}{ln(|s_1|)}) + n\pi}, n = 0, 1, 2, ...\alpha_{min} < \alpha_* < 1 \tag{18}$$

In the special case when $k = 1$ and $LC = 10^{-6}$, the value of $\alpha_* = 0.7356$ at which the poles are $s_* = -11461 \pm j3475$ as shown in Figure 8.

5. MAGNITUDE RESPONSE

For the fractional-order low-pass filter shown in Fig.1, the magnitude response is given by

$$\begin{aligned} G(j\omega, \alpha, \beta) \quad = \quad & [1 + \omega^{\alpha} RCcos(\frac{\alpha\pi}{2}) + \omega^{\alpha+\beta} LCcos(\frac{(\alpha+\beta)\pi}{2}). \\ & + j(\omega^{\alpha} RCsin(\frac{\alpha\pi}{2}) + \omega^{\alpha+\beta} LCsin(\frac{(\alpha+\beta)\pi}{2}))\Big]^{-1} \end{aligned} \tag{19}$$

$$|G(j\omega,\alpha,\beta)| = [1+2\omega^{\alpha}RCcos(\frac{\alpha\pi}{2})+2\omega^{\alpha+\beta}LCcos(\frac{(\alpha+\beta)\pi}{2}). \\ +\omega^{2\alpha}R^2C^2+\omega^{2\alpha+2\beta}L^2C^2+2\omega^{2\alpha+\beta}RLC^2cos(\frac{\beta\pi}{2})]^{\frac{-1}{2}} \quad (20)$$

Figure 9 shows the magnitude response of the fractional-order $RL_\beta C_\alpha$ circuit for different values of k. It is shown from this figure that as k is very small and $(\alpha+\beta)>1$ the response has peaks and these peaks vanish as k increases. For the first two subplots when $\beta=2\alpha=0.8$ and $\beta=3\alpha=1.2$, the systems are stable (unconditionally stable). However, as β increases, the peak values increase which shift the poles toward the unstable region of the s-plane. In addition, some of these cases have poles in the physical s-plane and some do not.

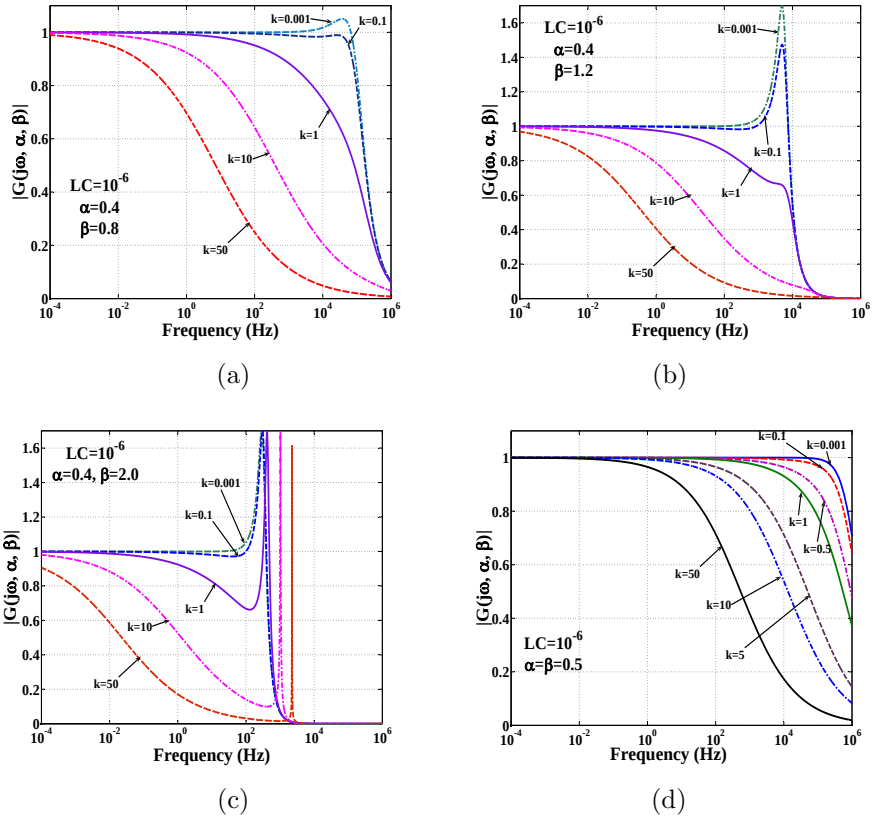

FIGURE 9. The magnitude response of the fractional-order LPF for different relationships between α and β

When $\beta=5\alpha=2.0$, the system becomes unstable as clear from its magnitude response shown in Figure 9(c) where the response has a huge peak for any value of k. In addition, Figure 9(d) shows the magnitude response in case $\alpha=\beta=0.4$ where the system doesnt have any peaks since no poles exist in the physical s-plane as verified before.

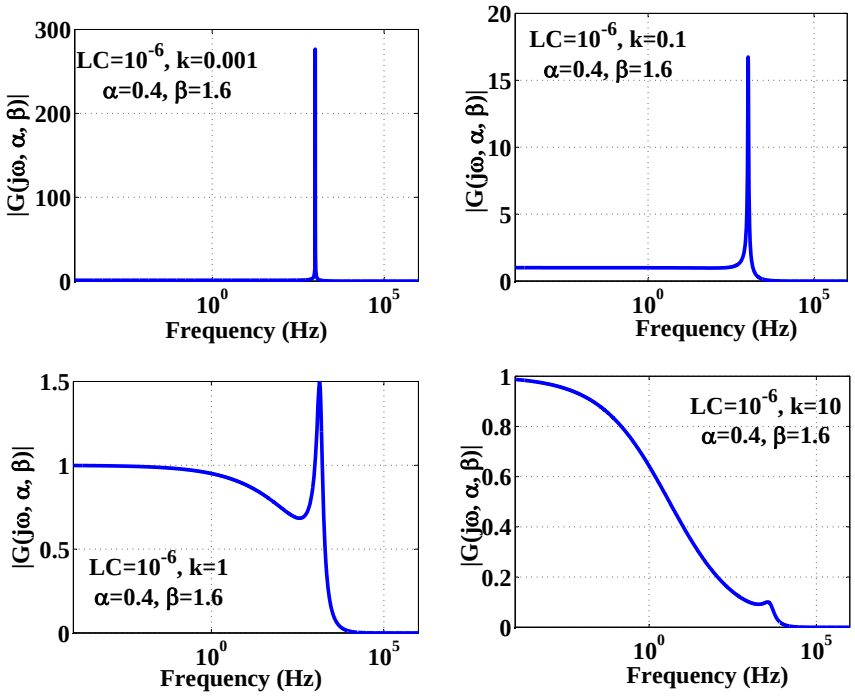

FIGURE 10. The magnitude response of the fractional-order LPF when $\beta = 4\alpha = 1.6$

Figure10 illustrates the behavior of the fractional-order LPF when $\alpha + \beta = 2.0$ where the system oscillates when $k = 0$ as shown from the first subplot. Note that all systems in Figure10 are stable and as k increases the poles move from the $\pm j\omega$ axis toward the stable region of s-plane. As k increases to 1.6 the peak of the magnitude response becomes smaller and the LPF effect appears. When $k = 1$, the peak has a reasonable value and as k becomes 10 these peaks almost vanish as shown in Figure10.

Conventionally, when the system oscillates, the magnitude response should be impulse as shown in Figure 10 when $k = 0.001$ where the system is very close to oscillate. Therefore, the peaks in Figures 9 and 10 reflect that the system is very close to the oscillation condition (may be from the stable side or from the unstable side). As long as the peak is high relative to other values, then systems poles are more close to the $j\omega$ axis. From Figure 9(b), when $\beta = 3\alpha = 1.2$ the system is stable when $k = 0.001$. However, for Figure 9(b) the system is unstable for all k when $\beta = 4\alpha = 2.0$.

6. PHASE RESPONSE

Similarly, the phase response of the $RL_\beta C_\alpha$ can be calculated from

$$tan(\angle G(j\omega, \alpha, \beta)) = \frac{\omega^\alpha RC sin(\frac{\alpha\pi}{2}) + \omega^{\alpha+\beta} LC sin(\frac{(\alpha+\beta)\pi}{2})}{1 + \omega^\alpha RC cos(\frac{\alpha\pi}{2}) + \omega^{\alpha+\beta} LC cos(\frac{(\alpha+\beta)\pi}{2})} \tag{21}$$

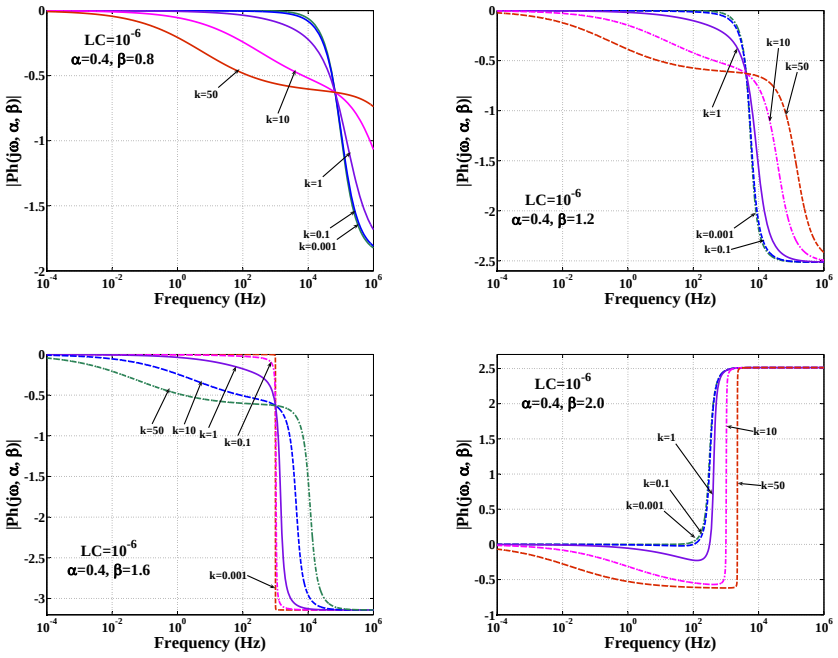

FIGURE 11. The phase response of the fractional-order LPF for different relationships of α and β

Figure 11 shows the phase response for $\beta = m\alpha = 0.4m$ where $m = 2, 3, 4$, and 5. The phase response begins at zero and as ω increases the phase reaches the value of $(-(\alpha+\beta)\pi/2)$ except in the unstable case shown in the last subplot $\beta = 5\alpha = 2.0$. In this case, as k tends to zero, the phase response changes from zero angle up to π suddenly which is the case of oscillation. However, in the case $\beta = 5\alpha = 2.0$ the system performance was abnormal since the phase goes down a little bit and then goes up to positive values which is unacceptable in the LPF systems. Therefore, Figure 11 discusses the response of four different cases

(1) Unconditionally stable with and without poles in the physical s-plane when $(\alpha, \beta) = (0.4, 0.8)$.
(2) Conditionally stable depends on the value of k but without oscillation when $(\alpha, \beta) = (0.4, 1.2)$.
(3) Conditionally stable depends on the value of k but with the possibility of oscillation when $(\alpha, \beta) = (0.4, 1.6)$.
(4) Unconditionally unstable when$(\alpha, \beta) = (0.4, 2.0)$.

7. CONCLUSION

In this paper, we studied the behavior of the conventional RLC in the fractional-order sense where two different orders are imposed for the inductor and the capacitor as $RL_\beta C_\alpha$. Stability analysis and the locations of poles in the physical s-plane are discussed with several cases showing four different scenarios. The first scenario where the system doesnt have any poles in the physical s-plane , the second scenario

where the poles exist in a confined range of k, the third scenario when the poles always exist in the physical s-plane independent of the value of k, and the final scenario when the poles exist in the physical s-plane with conditional stability according to the value of the parameter k. Several examples are introduced for these four scenarios including the oscillation condition and the limits of k for each scenario. The magnitude and phase response of the fractional-order LPF are also presented to verify the previous discussions.

References

[1] S. G. Samko, A. A. Kilbas and O. I. Marichev, Fractional integrals and derivatives: theory and application, Gordon and Breach, 1987.

[2] J. Sabatier, O.P. Agrawal and J.A. Tenreiro Machado, Advances in fractional calculus; theoretical developments and applications in physics and engineering, Springer, 2007.

[3] A. G. Radwan, A. S. Elwakil, and A. M. Soliman, Fractional-order Sinusoidal Oscillators: Design Procedure and Practical Examples, IEEE Trans. Circuits and Syst.-I, 55, 2051-2063, 2008.

[4] A. G. Radwan, A. S. Elwakil, and A. M. Soliman, On the generalization of second-order filters to fractional-order domain, Journal of Circuits Systems and Computers, 18, 2, 361-386, 2009.

[5] P. Melchior, B. Orsoni, O. Lavialle, and A. Oustaloup, The CRONE toolbox for Matlab: fractional path planning design in robotics, Laboratoire d'Automatique et de Productique (LAP) 2001. Copyright 2007 John Wiley and Sons, Ltd. Int. J. Circ Theor. Appl. 2008; 36:473–492 DOI: 10.1002/cta

[6] H. Li, Y. Luo, and Y. Q. Chen, A Fractional-order Proportional and Derivative (FOPD) Motion Controller: Tuning Rule and Experiments, IEEE Trans. Control Syst. Tech., 18, 2, 516- 520, 2010.

[7] R. L. Magin, Fractional calculus in bioengineering, Begell House, Connecticut, 2006.

[8] C. M. Ionescu and R. De Keyser, Relations Between Fractional-order Model Parameters and Lung Pathology in Chronic Obstructive Pulmonary Disease, IEEE Trans. On Biomedical Eng., 56, 4, 978- 987, 2009.

[9] A. Shamim, A. G. Radwan, K. N. Salama, Fractional Smith Chart Theory and Application, IEEE Microwave and Wireless Components Letters, 21, 3, 117- 119, 2011.

[10] A. G. Radwan, A. Shamim, K. N. Salama, Theory of Fractional-order Elements Based Impedance Matching Networks, IEEE Microwave and Wireless Components Letters, 21, 3, 120- 122, 2011.

[11] A. G. Radwan, K. Moaddy, Shaher Momani, Stability and Nonstandard Finite Difference Method of the generalized Chua's circuit, An International Journal of Computers and Mathematics with Applications, 62, 961970, 2011.

[12] Y. Yua, Han-Xiong Lib, The synchronization of fractional-order Rossler hyperchaotic systems, Physica A. 387, 13931403, 2008.

[13] A.M.A. El-Sayed, A.E.M. El-Mesiry, H.A.A. El-Saka, On the fractional-order logistic equation, Applied Mathematics Letters 20, 817823, 2007.

[14] Y. Q. Chen and K. L. Moore, Discretization Schemes for Fractional-order Differentiators and Integrators, IEEE Trans. Circuits and Syst.-I, 49, 3, 363-267, 2002.

[15] I. S. Jesus, T. J. A. Machado and B. J. Cunha, Fractional electrical impedances in botanical elements, Journal of Vibration and Control, 14, 9-10, 1389-1402, 2008.

[16] A.M.A. El-Sayed, A.E.M. El-Mesiry, H.A.A. El-Saka, Numerical solution for multi-term fractional -arbitrary- orders differential equations, Computational and Applied Mathematics 23, 1, 3354, 2004.

[17] K. Diethelm, N. J. Ford, Analysis of fractional differential equations, J. Math. Anal. Appl., 265, 229-248, 2002.

[18] A. G. Radwan, A. M. Soliman , A. S. Elwakil, and A. Sedeek, On the stability of linear systems with fractional-order elements, Chaos, Solitons and Fractals, vol. 40, 5, 2317-2328, 2009.

[19] Y. Q. Chen, A. Hyo-Sung, I. Podlubny, Robust stability check of fractional-order linear time invariant systems with interval uncertainties, Signal Processing, Vol. 86, 10, 2611-2618, 2006.

[20] G. W. Bohannan, S. K. Hurst, and L. Springler, Electrical component with fractional-order impedance, Utility Patent Application, US20060267595, 11/30/2006.
[21] G. W. Bohannan, Analog Realization of a Fractional Control Element - Revisited, Proc. of the 41st IEEE Int. Conf. on Decision and Control, Tutorial Workshop 2: Fractional Calculus Applications in Automatic Control and Robotics, 203-208, USA, 2002.
[22] G. Carlson, and C. Halijak, Approximation of fractional capacitors $(1/s)^{1/n}$ by a regular Newton process, IEEE Trans. Circuits and Syst, 11, 210-213, 1964.
[23] A. Abbisso, R. Caponetto, L. Fortuna, and D. Porto, Non-integer-order integration by using neural networks, Proceedings of International Symposium on Circuits and Systems, 38, 688–691, 2001.
[24] K. Saito, and M. Sugi, Simulation of power-law relaxations by analog circuits: fractal distribution of relaxation times and non-integer exponents, IEICE Trans. Fundam. Electron. Commun. Comput. Sci., E76(2), 205-209, 1993.
[25] M. Nakagawa, and K. Sorimachi, Basic characteristics of a fractance device, IEICE Trans. Fundam. Electron. Commun. Comput. Sci., vol. E75, no.12, pp. 1814-1819, 1992.
[26] K. Biswas, S. Sen, and P. Dutta, Realization of a constant phase element and its performance study in a differentiator circuits, IEEE Trans. Circuits and Syst.-II, vol. 53, pp. 802-806, 2006.
[27] T. C. Haba, G. L. Loum, G. Ablart, An analytical expression for the input impedance of a fractal tree obtained by a microelectronical process and experimental measurements of its non-integral dimension, Chaos, Solitons and Fractals, 33, 364373, 2007.

A. G. Radwan
Engineering Mathematics Department, Faculty of Engineering, Cairo University, Giza, 12613, Egypt.
Nanoelectronics Integrated Systems Center (NISC), Nile University, Cairo, Egypt.
E-mail address: agradwan@ieee.org